Chapter 1 Introduction

1.1 Laser Trapping: Basic Physical Principles

In 1970, Ashkin [1] reported that light forces could be used to manipulate the microscopic particles, when the momentum of the focused laser light is altered by the particle on being reflected, refracted or absorbed. The two basic light pressure forces were identified: a scattering force in the direction of the incident light beam, and a gradient force in the direction of the intensity gradient of the beam. It was shown experimentally that, using just these forces, one could accelerate, decelerate, and even stably trap small micro-sized neutral particles using focused laser beam. This led to the discovery of stable optical trapping and manipulation of small neutral particles. Latter work on understanding of similar scattering and gradient light forces on atoms led to the first experiment on focusing and defocusing of atoms by light and the invention of the single beam gradient or tweezers trap for atoms. By 1980 the fundamentals of the field had been established [2]. Until now, optical tweezers has been applied in the field of bioscience, colloidal sciences [3], and microfluidic studies [4].

1.1.1 Particle Trapping

Optical trapping for microscopic dielectric particles by a single beam gradient force trap was first demonstrated in 1986 by A. Ashkin [5]. As recently theoretical and experimental researches have reported, broadly the ideal model of trapping is dependent on the relation of laser wavelength and size of particle. If the size of particle exceeds laser wavelength, means at Mie scattering regime, the theoretical model is commonly *Ray Optics Model*. In the contrast, the situation that laser wavelength exceeds the size of particle trapped is dealt with *Electromagnetic Model*, at Rayleigh scattering regime. We will roughly discuss these models in the following.

(1) Ray Optics Model: this condition is applied when the size of particle is larger than wavelength of laser beam. According to the electromagnetic theory that suggesting photons carries energy and momentum and Newton's theory that every action has equal and opposite reaction, the basic trapping theory is obtained in ray optical treatment. Due to Snell's law in ray optics, the refractive indices of inner particle (n_1) and the surrounding medium (n_2) are quite important for ray tracing. Therefore, the three trapping force conditions included $n_1 > n_2$, $n_2 > n_1$, and high refractive particles are plotted in Figure 1.1(a), (b), and (c), respectively.

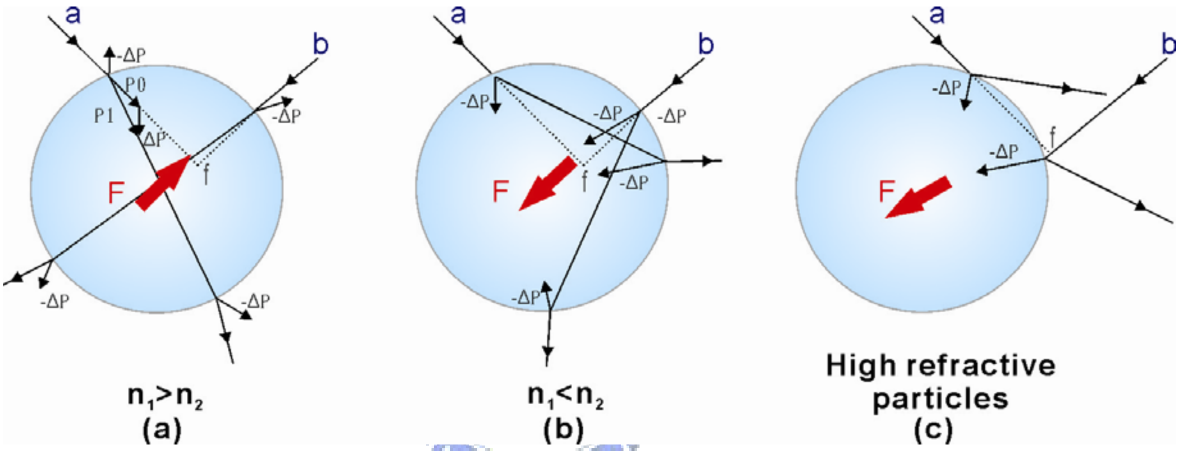

Fig. 1.1 Optical force on a dielectric particle by a focused laser beam.

The point *f* is the focus spot of incident ray light *a*, *b*. In figure 1-1(a), the refraction of a light ray by a spherical particle n_1 in the medium of n_2 leads to a light momentum change, $\triangle P=P_1-P_0$, where P_0 and P_1 are light momentum before and after refraction, respectively. $\triangle P$ should be exerted to the particle with the direction opposite to $\triangle P$, means $-\triangle P$. At the same situation of each ray light, the summation of $-\triangle P$ at each point of the particle contacted incident light will induce the radiation force *F*. The force *F* can be decomposed to axial and trans-axial components. Therefore the particle is optically trapped or levitated in the vicinity of the focal point of the focus laser beam. For the same reason, if refractive index of the particle is larger than the surrounding medium's, the focused laser beam will induce the repulsive radiation force F at the opposition direction from Figure 1.1(a), shown in Figure 1.1(b). The optical force situation of high refractive particles is the same as Figure 1.1(c). Based on the above discussions, the spatial distribution of focused laser-beam intensity and the relevant potential of the radiation force are schematically shown in Figure 1.2. From the diagram, the high-refractive index particle can be trapped by focused laser beam. Otherwise the low-refractive index or high refractive particles must be trapped by circular scanning focused beam, or hollow beam [6].

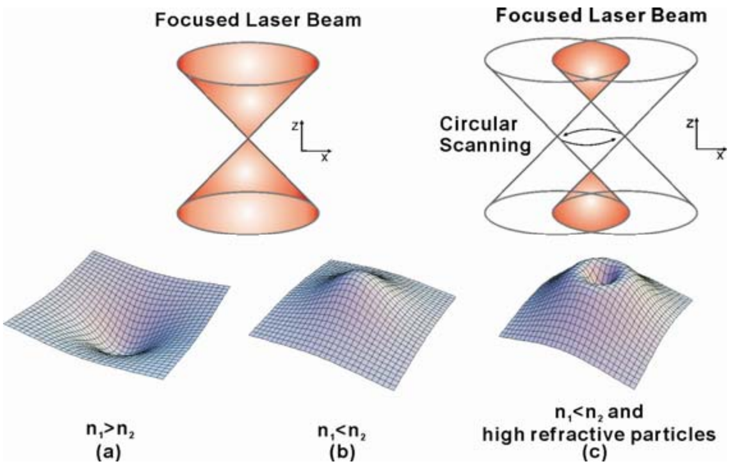

Fig. 1.2 Schematic representation of the spatial distribution of trapping force from a focused laser.

(2) Electromagnetic Model: this condition is satisfied when size of the particle is smaller than the wavelength of incident laser beam, means at Rayleigh scattering regime. The dielectric particle is too small that incident light would induce the dipole on it. Under this condition the particle is treated as an induced small dipole immersed in an optical field, the forces acting on this dipole would be dependent on the central frequency of incident light. And the details will be discussed in next subsection: *Atom Trapping*.

1.1.2 Atom Trapping

For neutral atoms, it has become experimental routine to produce ensembles in the microkelvin region, and various experiments are being performed with such laser-cooled ultracold gases. The basic concepts of atom trapping in optical dipole potentials result from the interaction with *far-detuned* light. In this case of particular interest, the optical excitation is very low and the radiation force due to photon scattering is negligible as compared to the dipole force. The basic model of optical dipole trapping is considering the atom as a simple oscillator subject to the classic radiation field. When an atom is placed into laser light, the electric field E induces an atomic dipole momentum $\boldsymbol{p}$, can be shown as [7]

$$\tilde{p} = \alpha \tilde{E} . \quad (1.1.1)$$

Here α is the complex polarizability, which depends on the driving frequency ω. The interaction potential of the induced dipole moment p in the driven field E are given by

$$U_{dip} = -\frac{1}{2}\langle pE \rangle = -\frac{1}{2\varepsilon_0 c} Re(\alpha) I(r), \quad (1.1.2)$$

where the angular brackets denote the time average over the rapid oscillating terms, the field intensity is $I = 2\varepsilon_0 c |\tilde{E}|^2$, c is the speed of light and ε_0 is the permittivity of the free space. The equation of the motion for the driven oscillation of the electron is shown as

$$m_e \ddot{x} + m_e \Gamma_\omega \dot{x} + m_e \omega_0^2 x = -eE(t) . \quad (1.1.3)$$

The permittivity parameter would be calculated straightforwardly as

$$\alpha = \frac{e^2}{m_e} \frac{1}{\omega_0^2 - \omega^2 - i\omega\Gamma_\omega} . \quad (1.1.4)$$

By introducing the on-resonance classical damping rate $\Gamma_\omega = \frac{e^2\omega^2}{6\pi\varepsilon_0 m_e c^3}$ and $\Gamma \equiv \Gamma_{\omega_0} = (\omega_0/\omega)^2 \Gamma_\omega$, the permittivity would be simplified as

$$\alpha = 6\pi\varepsilon_0 \frac{\Gamma/\omega_0^2}{\omega_0^2 - \omega^2 - i(\omega^3/\omega_0^2)\Gamma} . \quad (1.1.5)$$

Then we can obtain the dipole potential and scattering rate in the relevant case of large detuning and negligible saturation as

$$U_{dip}(r) = -\frac{3\pi c^2}{2\omega_0^3}\left(\frac{\Gamma}{\omega_0 - \omega} + \frac{\Gamma}{\omega_0 + \omega}\right) I(r) . \tag{1.1.6}$$

In most experiments, the laser is tuned relatively close to the resonance at ω_0 such that the detuning $\Delta \equiv \omega\text{-}\omega_0$ fulfills $|\Delta| << \omega_0$, the dipole potential and scattering rate simplify to

$$U_{dip}(r) = \frac{3\pi c^2}{2\omega_0^2}\frac{\Gamma}{\Delta} I(r) . \tag{1.1.7}$$

Moreover, the equation (1.1.7) shows one very essentially point for dipole trapping:

Sign of detuning: Below an atomic resonance ($\Delta < 0$, *red-detuning*) the dipole potential is negative and the interaction thus attracts atoms into the light field. Potential minima are therefore found at positions with maximum intensity. Above resonance ($\Delta > 0$, *blue-detuning*) the dipole interaction repels atoms out of the field, and potential minima correspond to minima of the intensity. According to the distinction, dipole traps can be divided into two main classes, *red-detuned traps* and *blue-detuned traps*.

Based on this result, the required light fields of both red-detuned dipole trap ($\Delta < 0$) and blue-detuned dipole trap ($\Delta > 0$) for atoms are quiet different. Figure 1.3 is the illustration of dipole traps with red and blue detuning. In the first case, a simple Gaussian laser beam is assumed. In the second case, a Laguerre-Gaussian LG_{01} "doughnut" mode is chosen with which provides the same potential depth and the same curvature in the trap center.

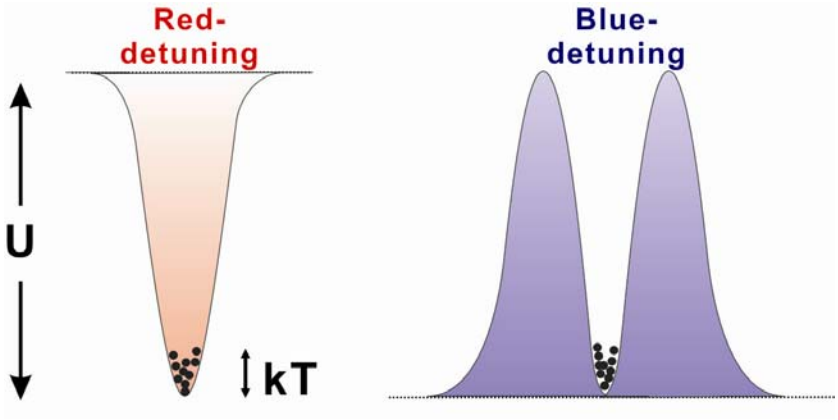

Fig. 1.3 Illustration of dipole traps with red and blue detuning.

Within the refractive index of atom verse incident light frequency from permittivity can be plotted in Figure 1.4. With blue-detuning light, the refractive index of atom would be smaller than 1 (environment), and red-detuning light is in contrariwise.

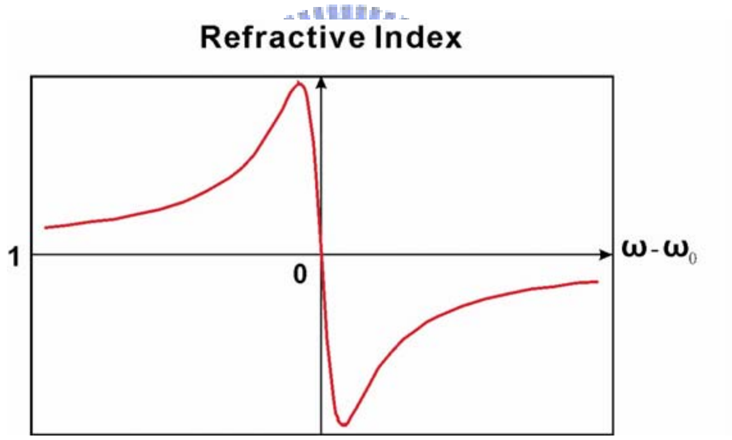

Fig. 1.4 The refractive index of atom versus incident light frequency.

In conclusion, this obviously implies that "doughnut" or hollow beam is used to trap particles of low refractive index and Gaussian beam is used to trap particles of high refractive index. Besides, the frequency-detuning light field would be considered to obtain in Rayleigh particle or atom trapping.

1.2 Optical Bottle Beam

Optical bottle beam [8] or optical hollow beam [9] that contains a null intensity point or a sequence of points along the propagation direction has applications in optical tweezers for trapping micro-particles of low index [10]. The micro-particles of low index are trapped in minimum intensity regions or central dark regions by repulsive force of beam. For the three dimensional shape of dark region which trapped particles with propagation is similar to a bottle shown in Figure 1.5 [11], it was denominated as optical bottle beam. Recently, optical self-imaged bottle beam could be provided three dimensional trapping potential for high- and low-index microparticles at constructive and destructive interference points, respectively [12]. Optical bottle beam was initially generated by interfering Laguerre-Gaussian (LG) beams with different radial mode index at the common focus in such a manner that the on-axis intensity at the focus is zero to form three-dimensional dark spot. For the three-dimensional dark region, optical bottle beam is not the same as the two dimensional confinement of Bessel beam. Recently, the generations of optical bottle beam included using holographic phase plate [13], spatial light modulator [14], obtaining directly from laser cavity [15] [16], and combination of axicon and a lens [17]. From combination of axicon and a lens, its conversion to hollow beam by changing the relative distance between them was also reported [17].

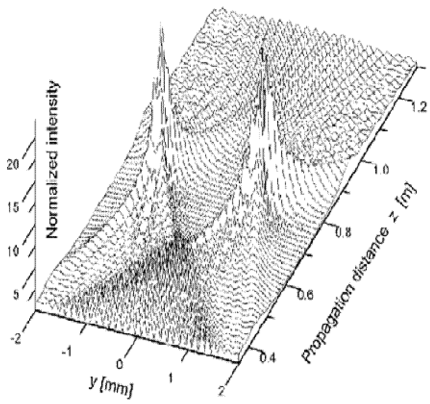

Fig. 1.5 Diagram of Optical bottle beam.

1.3 Supercontinuum Generation

Supercontinuum generation is the formation of broad continuous spectra by propagation of high intensity pulses through nonlinear media, and was first observed in 1970 by Alfano and Shapiro [18]. Its spectral range is broad enough to cover the visible region, even into the infrared spectral range. This generation is a complex nonlinear process, as the wavelength of the output phonons is different from that of the input laser phonons. Provided enough intensity is available, supercontinuum generation can be observed in a drop of water. However, the nonlinear effects involved in the spectral broadening are highly dependent on the dispersion of the media, and a clever dispersion design can significantly reduce the input power required. The widest spectra are obtained when the pump pulses are launched close to the zero-dispersion wavelength of the nonlinear media, especially in the anomalous dispersion region. Therefore, recently the microstructured fibers (MFs) have been attracted to become powerful tools that generated the SC due to the adjustable zero-dispersion wavelength was first demonstrated in 1999 [19]. It's because the zero-dispersion profile of MFs can be shifted by fabricated the structures of fiber, e.g., core diameter, hole-diameter, or other structure parameters. In order to generate the SC in MFs, the high power input source is generally femtosecond [20] [21] or picosecond mode-locked laser system [26].

Due to the high peak power and short duration of femtosecond pulse laser, it is easily to induce strong nonlinear effects in MFs. And these nonlinear effects included high-order soliton breakup [22], self-frequency shift [23], and degenerate four-wave mixing [24]. Usually about mini-watts of average pumping are needed to generating the SC in the femtosecond mode-locked laser system. The common and general experiment for generating the SC is the combination of Ti: sapphire mode-locked femtosecond laser system with the microstructured fibers. Supercontinuum source is a new type of light source that provides a combination of these desirable features: high output power, a broad, flat spectrum, and a high degree of spatial coherence that allows tight focusing. In applications such as optical coherence tomography [25] [29], optical frequency metrology [27] [28], photon device testing, and optical communication can be made.

1.4 Advantages of White Light Optical Trapping

Recently, optical tweezers for supercontinuum white light is a novel interesting biological technique to be developed rapidly. The two unique features of supercontinuum or white light generated from microstructured fiber are its high spatial coherence and extremely broad bandwidth. Because of its high spatial coherence, supercontinuum white light that is similar to a normal laser light can be focused to a tiny spot or collimated to pass through optical elements. On the other hand, the broad bandwidth of supercontinuum white light increases its information capacity and offers new opportunities for next generation optical information systems. White light tweezes open up the unique possibility of characterizing a microscopic object while it is being three-dimensionally trapped and manipulated [30]. The strong optical scattering spectrum would be depends on structure of the trapped object while trapped. Through optical spectroscopy, researchers can probe the trapped particle's sizes, shape, refractive index and chemical compositions. Besides, the feature on broad bandwidth of white light is expected to enhance optical guiding distance compared to a monochromatic continuous laser and a femtosecond Gaussian laser due to the elongation of the focus for the supercontinuum source [31]. The numerical calculations of axial and radial forces for a SC sustained over a longer distance support this fact.

Due to the unique features of supercontinuum white light, the application in optical tweezers is novel and worth to be expected. However, the whole recent researches of optical tweezers for supercontinuum white light are about focused light trapping on micro-sized particles. In this work, the research about generation of supercontinuum white light optical bottle beam was first discussed and investigated. Future works of trapping application and advantage on white light bottle beam would be gradually investigated. From a new type of white light bottle beam trapping, hope it can be developed for atom trapping needed frequency-detuning light or particle trapping of low refractive index Mie particles on experiments.

1.5 Organization of this Thesis

In Chapter 2, we will introduce the theory about the numerical calculation of bottle beam and generated concepts of SC in MFs. The content describes two diffraction theory, scalar diffraction (Fresnel-Kirchhoff's formula) and vectorial diffraction (vectorial Rayleigh diffraction) to discuss the bottle range and its vectorial field. In Chapter 3, we will introduce our experiment to generate SC white light bottle beam in detail, including laser system, the microstructured fiber and monitoring the SC optical bottle beam. Then, we will compare the results of experiment and theoretical calculation in Chapter 4 and distribution profile of bottle beam. For the influence of the longitudinal field by focusing the beam would be considered and important, Chapter 5 is our simulation on vectorial field of bottle beam by assuming radial or linear polarization input. Finally, we will give a conclusion and the future works in Chapter 6.